NUSC Report No. 4169

Spectral Estimation by Means of Overlapped Fast Fourier Transform Processing of Windowed Data

ALBERT H. NUTTALL
Office of the Director of Science and Technology

13 October 1971

NAVAL UNDERWATER SYSTEMS CENTER

ABSTRACT

An investigation of power-density autospectrum estimation by means of overlapped Fast Fourier Transform (FFT) processing of windowed data is conducted for four candidate spectral windows with good side-lobe behavior. A comparison of the four spectral windows is made on the basis of equal half-power resolution bandwidths. The criteria for comparison are: (1) statistical stability of the spectral estimates, (2) leakage (side lobes) of the spectral windows, (3) number of FFTs (number of overlapped pieces) required, and (4) size of each FFT required. The dependence of these criteria on the amount of overlap is investigated quantitatively.

Some striking invariances are discovered. Specifically, it is shown that the ultimate variance-reduction capabilities of the four windows, as measured by the equivalent number of degrees of freedom (EDF), are virtually identical under the constraint of equal half-power bandwidths. Furthermore, when the proper overlap is used for each window, the stability of this method of spectral estimation is identical to that of the "indirect" correlation approach. Also, the number of FFTs required to realize 99 percent (or less) of the maximum EDF is virtually independent of the particular window employed. The required fractional overlap of the four data windows for 99 percent (or less) of the maximum EDF is virtually independent of the product of the available time and the resolution bandwidth, although it does depend on the particular window. Tables of required overlap are presented. The only tradeoff among the four windows is that those with better side lobes require larger-size FFTs. All of these results are derived for a Gaussian random process, under the assumption that the resolution bandwidth of the spectral window is smaller than the finest detail in the true spectrum.

Rules of thumb for the maximum EDF and the number of FFTs required to realize 99 percent of the maximum EDF are given. The possibility of weighting individual spectral estimates unequally in order to optimize the EDF is investigated; the gain is found to be negligible for cases of practical interest.

ADMINISTRATIVE INFORMATION

This work was performed under NUSC Project No. A-041-00-00, and Navy Subproject No. ZF XX 112 001, "Applications of Statistical Communication Theory to Target Detection and Classification," Principal Investigator, Dr. A. H. Nuttall, Code TC. The sponsoring activity is Chief of Naval Material, Program Manager, Dr. J. H. Huth.

The technical reviewer for this report was Dr. D. W. Hyde, Code TC.

REVIEWED AND APPROVED: 13 October 1971

W. A. Von Winkle

W. A. Von Winkle
Director of Science and Technology

Inquiries concerning this report may be addressed to the author via Officer in Charge, New London Laboratory, Naval Underwater Systems Center, New London, Connecticut 06320

DOCUMENT CONTROL DATA - R & D

Naval Underwater Systems Center
Newport, Rhode Island 02840

UNCLASSIFIED

SPECTRAL ESTIMATION BY MEANS OF OVERLAPPED FAST FOURIER TRANSFORM PROCESSING OF WINDOWED DATA

Research Report

Albert H. Nuttall

13 October 1971	48	13
A-041-00-00 ZF XX 112 001	4169	

Approved for public release; distribution unlimited.

Department of the Navy

An investigation of power-density autospectrum estimation by means of overlapped Fast Fourier Transform (FFT) processing of windowed data is conducted for four candidate spectral windows with good side-lobe behavior. A comparison of the four spectral windows is made on the basis of equal half-power resolution bandwidths. The criteria for comparison are: (1) statistical stability of the spectral estimates, (2) leakage (side lobes) of the spectral windows, (3) number of FFTs (number of overlapped pieces) required, and (4) size of each FFT required.

Some striking invariances are discovered in the ultimate variance-reduction capabilities and in the number of FFTs required to realize 99 percent (or less) of the maximum EDF. The only trade-off among the four windows is that those with better side lobes require larger-size FFTs.

DD FORM 1473

KEY WORDS	LINK A		LINK B		LINK C	
	ROLE	WT	ROLE	WT	ROLE	WT
Spectral estimation						
Fast Fourier Transform						
Windowed data						
Statistical bandwidth						
Half-power bandwidth						
Stationary random processes						
Short modified periodograms						

TABLE OF CONTENTS

REVERSE BLANK

LIST OF FIGURES

REVERSE BLANK

LIST OF TABLES

GLOSSARY

T	available record length
B	desired frequency resolution, half-power bandwidth
x	random process
t	time
f, f_1	frequency
G	power-density spectrum of process x
w	data window
L	segment length
S	shift of data windows
P	number of pieces; number of FFTs
p	integer in range (1, P)
Y_p	Fourier transform of weighted p-th piece
$\hat{G}$, $\tilde{G}$	estimate of power density
Δt	sampling increment of x
W	Fourier transform of w
$\|W\|^2$, Q_i	spectral window
$E\{A\}$	statistical average of A
$Var\{A\}$	variance of A
ϕ_w, ϕ_u	correlations of data windows w, u

K, K_w	equivalent degrees of freedom
u	normalized data window
B_{st}	statistical bandwidth
C_{st}	statistical-bandwidth constant
U	Fourier transform of u
$\mathrm{sinc}(x)$	$\sin(\pi x)/(\pi x)$
C	half-power-bandwidth constant
N_s	number of samples in segment length
w_p	weighting applied to $\lvert Y_p \rvert^2$
R	correlation of process x
γ_k	correlation of weights $\{w_p\}$
M_k	normalized correlation(Eq. (C-6))
χ	ambiguity function of data window w

Abbreviations

FFT	Fast Fourier Transform
EDF	Equivalent Degrees of Freedom
max	Maximum
FO	Fractional Overlap

SPECTRAL ESTIMATION BY MEANS OF OVERLAPPED FAST FOURIER TRANSFORM PROCESSING OF WINDOWED DATA

INTRODUCTION

Estimation of the power-density spectra of stationary random processes is an important problem and occurs frequently in many fields. The resolution of closely spaced frequency components, with limited amounts of data, presents inherent limitations on the statistical stability of the estimates. Also, the prevention of leakage of undesired frequency components into the frequency being analyzed dictates a careful choice of data weighting. Lastly, the extent and complexity of the data processing required to realize the desired resolution, stability, and leakage control are important considerations.

The fundamental, conflicting desires involved in spectral estimation become painfully obvious when the amount of data available for analysis is limited and can not be augmented by additional measurements. For example, the available record length may be limited by

a. nonstationary conditions (changing environment),

b. storage limitations,

c. equipment failure, and

d. time-sharing requirements.

Although factors b, c, and d can often be remedied or corrected, factor a often can not be controlled. Thus, only a small segment of the time record may be usable for each spectral analysis. If fine frequency resolution is desired, the limited number of independent observations available makes stable estimation impossible in some cases. One must then be willing to accept coarser, but more stable, spectral estimates.

The two fundamental parameters that control the performance of spectral estimation are the available record length, T, in which the sample of the random process is assumed stationary, and the desired frequency resolution, B, of the spectral analysis. Large values of the fundamental BT product yield good performance of the analysis technique, but small values are often forced upon us by too small a record length T or too fine a desired resolution B. The problem here is to make maximum use of the available data.

Spectral analysis has received much attention in the past [1-6], especially since the advent of the Fast Fourier Transform (FFT) [7, 8]. In particular, the method of averaging short modified periodograms [9] is a prime candidate for spectral analysis — for several reasons. First of all, nonstationary trends in the data are more readily observable through the time-local spectral estimates of each segment. Second, the size of each FFT can be kept reasonably small, thereby reducing storage, execution time, and round-off error. Third, the frequency resolution is easily controlled by the choice of segment length, and leakage (side lobes) can be controlled by the proper choice of window in the time domain. Lastly, overlapped segments of windowed data utilize more fully the variance-reduction capability of a given record length.

The problem to be addressed here has to do with the choice of window and amount of overlap to employ for a particular application. Specifically, if we employ a window with very small spectral side lobes, how much should the segments be overlapped, and does the overlap vary greatly with the particular window selected? (Fifty-percent overlap has been suggested as a reasonable procedure for the triangular data window [9, p. 72].) How many FFTs of what size have to be performed for the different windows? Is the variance-reduction capability dependent on the particular window?

Four windows will be investigated. They are called data windows in the time domain, where they are multiplied by the available data record; they will be called spectral windows in the frequency domain, where their main effect enters via convolution. The four data windows are called triangular, cosine,* quadratic, and cubic and will be documented in a later section. Hamming weighting [2, p. 14], although it possesses good adjacent side lobes, is not considered here because the spectral window decays very slowly with frequency, thereby responding to frequencies far removed from the analysis band of interest.

PROBLEM DEFINITION

Consider that stationary random process x has been observed for a time interval T seconds; that is, $x(t)$ for $0 < t < T$ is available. Let the power-density autospectrum of this process at frequency f be denoted by $G(f)$, where double-sided spectral notation will be employed. We wish to estimate spectrum G with a resolution of B hertz, where B is the half-power (-3 dB) bandwidth of the desired resolution.

*Also called Hanning weighting.

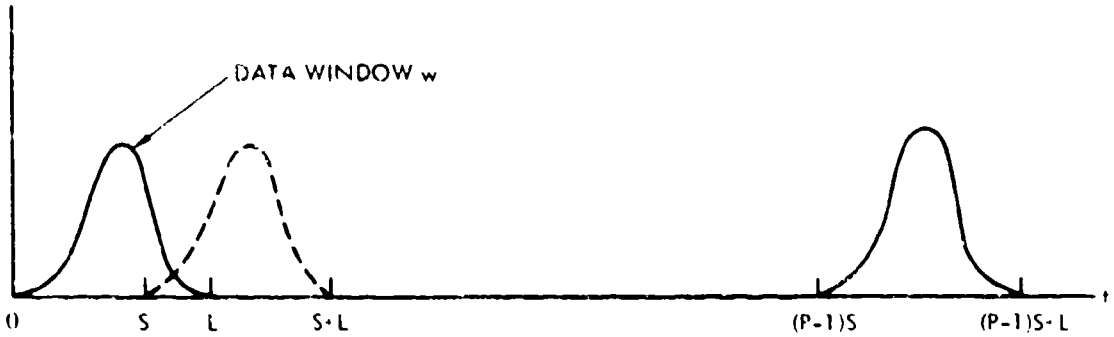

Fig. 1. Overlapped Data Windows

The method of obtaining the spectral estimates is depicted in Fig. 1. A data window w of duration L seconds is applied successively to the available data x in the overlapping intervals (0, L), (S, S+L), ... , ((P-1)S, (P-1)S+L). S is the amount of shift each adjacent data window undergoes, and P is the total number of pieces or segments employed. Since only T seconds of data are available, we must have

$$(P-1)S+L \leq T . \tag{1}$$

The segment length L should be large enough that the correlation function of process x is effectively zero for delays larger than L/2. (The relation between frequency resolution B and segment length L is discussed quantitatively later.) The form of the data window, depicted in Fig. 2, is even about the origin and real. Also, w(t) is zero for $|t| > L/2$.

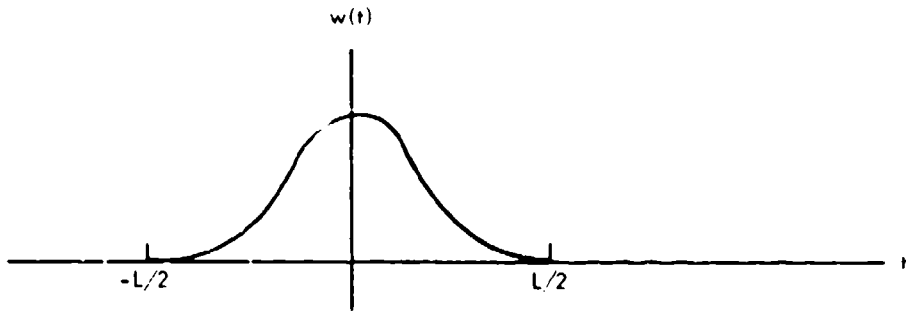

Fig. 2. Data Window

When the overlap in Fig. 1 is a significant fraction of the segment length, the effective use of the available data x is fairly uniform over the entire interval T except for the edges of the data, where a gradual taper over an interval of length $L/2$ takes place. This is consistent with earlier suggestions [10, p. 58] for maximum use of the available data. Notice that the percentage of taper depends on the desired frequency resolution and available record length, and is not a constant, such as 10 percent, as has occasionally been suggested.

The estimate of the power-density spectrum G is obtained as follows. First, a Fourier transform on the p-th windowed section is performed*:

$$Y_p(f) = \int dt\, \exp(-i2\pi ft)\, x(t)\, w\left[t - \frac{L}{2} - (p-1)S\right], \qquad 1 \le p \le P. \tag{2}$$

The spectral estimate at frequency f is then available as the average of the P pieces:

$$\hat{G}(f) = \frac{1}{P} \sum_{p=1}^{P} \left|Y_p(f)\right|^2 . \tag{3}$$

Equation (2) assumes a continuous, rather than discrete, form of signal processing [2, Secs. 4-11 versus 12-21]. However, if the discrete version of Eq. (2), where samples of x are taken Δt seconds apart, is such that aliasing is negligible, there is little difference between the two methods of spectral analysis [2, pp. 37-39 and 123-125]. We shall assume that Δt is so chosen and confine attention here to the continuous processing technique of Eq. (2). Of course, in practice, Eq. (2) is approximated by a discrete Fourier transform [9, p. 70], in which case dc and linear-trend removal should be considered for the sampled data [2, pp. 47-49].

The spectral estimate $\hat{G}(f)$ in Eq. (3) is a random variable. Its mean and variance are evaluated in Appendix A under the assumptions that x is a Gaussian random process and that the frequency resolution of the spectral window $|W|^2$, where

$$W(f) = \int dt\, \exp(-i2\pi ft)\, w(t), \tag{4}$$

is narrower than the finest detail in the true spectrum G. (This latter assumption is equivalent to that given under Eq. (1) for segment length L.) The results are

*Integrals without limits are over the range of non-zero integrand.

$$E\{\hat{G}(f)\} = \int d\nu\ G(f-\nu)\ |W(\nu)|^2 \cong G(f) \int d\nu\ |W(\nu)|^2 , \tag{5}$$

$$\mathrm{Var}\{\hat{G}(f)\} \cong \frac{1}{P} \sum_{k=-(P-1)}^{P-1} \left(1 - \frac{|k|}{P}\right) \left| \int d\mu\ \exp(i2\pi\mu kS)\ G(\mu)\ |W(f-\mu)|^2 \right|^2$$

$$\cong G^2(f)\, \frac{1}{P} \sum_{k=-(P-1)}^{P-1} \left(1 - \frac{|k|}{P}\right) \left|\phi_w(kS)\right|^2 , \tag{6}$$

where

$$\phi_w(\tau) = \int dt\ w(t)\ w^*(t - \tau) . \tag{7}$$

Relation (5) shows that the mean of the spectral estimate is equal to the convolution of the true spectrum G with the spectral window $|W|^2$. Relation (6) expresses the variance of the spectral estimate in terms of the number of pieces P, the shift S, and the autocorrelation ϕ_w of the data window. The result, Eq. (6), holds if f is greater than the bandwidth of the spectral window; the right side of Eq. (6) must be doubled if $f = 0$ [see also 9, p. 71].

The equivalent number of degrees of freedom (EDF) in spectral estimate $\hat{G}$ is defined as [2, p. 22]

$$K = 2\, \frac{E^2\{\hat{G}(f)\}}{\mathrm{Var}\{\hat{G}(f)\}}$$

$$= \frac{2P}{\displaystyle\sum_{k=-(P-1)}^{P-1} \left(1 - \frac{|k|}{P}\right) \left| \frac{\phi_w(kS)}{\phi_w(0)} \right|^2} , \tag{8}$$

employing Eqs. (4) through (6). Notice that under the assumptions given above, K is independent of the value of frequency f and true spectrum G; for $f = 0$, K is given by one half of Eq. (8).

For computational purposes, it is convenient to define a normalized data window u according to

$$u(x) = w(Lx) . \tag{9}$$

Then u contains the shape information of data window w but extends only over the interval (-1/2, 1/2). It follows that

$$\phi_w(\tau) = L\ \phi_u(\tau/L)\ , \tag{10}$$

where

$$\phi_u(\tau) = \int dt\ u(t)\ u^*(t-\tau)\ . \tag{11}$$

The EDF in Eq. (8) then becomes

$$K = \frac{2P}{\sum_{k=-(P-1)}^{P-1} \left(1 - \frac{|k|}{P}\right) \left| \frac{\phi_u(kS/L)}{\phi_u(0)} \right|^2}\ . \tag{12}$$

In order to minimize the fluctuations in the spectral estimate $\hat{G}$, we should maximize K in Eq. (12). To accomplish this for a given number of pieces P and segment length L the shift S in Eq. (12) should be chosen as large as possible so that ϕ_u is as small as possible at S/L, 2S/L, etc. However, since Eq. (1) dictates a constraint among these variables, the best choice of shift S — for given record length T, number of pieces P, and segment length L — is given by equality in Eq. (1):

$$S = \frac{T-L}{P-1} \quad (\text{for } P \geq 2)\ . \tag{13}$$

Substituting Eq. (13) in Eq. (12), we have

$$K = \frac{2P}{\sum_{k=-(P-1)}^{P-1} \left(1 - \frac{|k|}{P}\right) \left| \frac{\phi_u\left(k \frac{\frac{T}{L} - 1}{P - 1}\right)}{\phi_u(0)} \right|^2}\ . \tag{14}$$

Equation (14) expresses the EDF as a function of

P, number of pieces in the average,

T/L, ratio of record length to segment length, and

ϕ_u, autocorrelation of shape of data window.

The problem now is to maximize the EDF in Eq. (14) by choosing, subject to specified record length T and desired half-power frequency resolution B, the number of pieces, P, for several data windows, w. It will turn out that the optimum value for P is not infinite.

One special case of Eq. (14) is worth comment: if $P \leq T/L$, the values of ϕ_u in Eq. (14) are zero since u extends only over (-1/2, 1/2). Then K equals 2P, that is, regardless of the window, the EDF increases linearly with the number of pieces P until overlap occurs (see Eq. (13)). As P increases somewhat beyond T/L, K continues to increase, although at a slower rate, because the overlapped pieces are progressively more statistically dependent. Of importance in the behavior of K are the rate of increase of K with P, and the maximum value of K attainable through the choice of P.

LIMITING VALUE OF EQUIVALENT NUMBER OF DEGREES OF FREEDOM

As the number of pieces P tends to infinity, the overlap approaches 100 percent, and the denominator of Eq. (14) approaches an integral, yielding

$$K_w \equiv \frac{2}{\int_{-1}^{1} dx\,(1-|x|)\left|\frac{\phi_u\left(\left(\frac{T}{L}-1\right)x\right)}{\phi_u(0)}\right|^2}$$

$$= \frac{2\left(\frac{T}{L}-1\right)}{\int_{-\frac{T}{L}+1}^{\frac{T}{L}-1} d\tau\left(1-\left|\frac{\tau}{\frac{T}{L}-1}\right|\right)\left|\frac{\phi_u(\tau)}{\phi_u(0)}\right|^2}. \qquad (15)$$

This limiting value depends only on T/L and the correlation ϕ_u of the shape u of the window. It is finite because the overlapped pieces are statistically dependent.

For large values of T/L (ratio of record length to segment length), an alternate form of Eq. (15) is very illuminating. If Eq. (10) is utilized, the denominator approaches

$$\int d\tau \left| \frac{\phi_u(\tau)}{\phi_u(0)} \right|^2 = \int d\tau \left| \frac{\phi_w(L\tau)}{\phi_w(0)} \right|^2 = \frac{1}{L} \int dt \left| \frac{\phi_w(t)}{\phi_w(0)} \right|^2 ; \tag{16}$$

but from Eqs. (7) and (4),

$$\phi_w(0) = \int dt \, |w(t)|^2 = \int df \, |W(f)|^2 , \tag{17}$$

and

$$\phi_w(t) = \int df \, \exp(i2\pi ft) \, |W(f)|^2 , \tag{18}$$

giving

$$\int dt \, |\phi_w(t)|^2 = \int df \, |W(f)|^4 \tag{19}$$

by Parseval's Theorem. Combining Eqs. (15) through (19), we obtain

$$K_{(1)} \cong 2 \, (T - L) \frac{\left[\int df \, |W(f)|^2 \right]^2}{\int df \, |W(f)|^4} , \quad \text{for } \frac{T}{L} \gg 1 . \tag{20}$$

If we define the statistical bandwidth [5, p. 265] of spectral window $|W|^2$ as

$$B_{st} = \frac{\left[\int df \, |W(f)|^2 \right]^2}{\int df \, |W(f)|^4} \equiv \frac{C_{st}}{L} , \tag{21}$$

then

$$K_{(1)} \cong 2 \, (T - L) \, B_{st} = 2 \left(\frac{T}{L} - 1 \right) C_{st} , \quad \text{for } \frac{T}{L} \gg 1 . \tag{22}$$

The constant C_{st} is dimensionless and of the order of unity; it depends only on the shape of the window:

$$C_{st} = \frac{\left[\int df\, |U(f)|^2\right]^2}{\int df\, |U(f)|^4}, \tag{23}$$

where U is the Fourier transform of u (see also Eq. (9)).

The first form in Eq. (22) for K_{∞} indicates that if windows are compared on the basis of equal statistical bandwidths (by appropriate choice of segment length L for each data window), then all windows have the same value of K_{∞} for large T/L; that is, all windows have the same variance-reduction capability, when compared on the basis of equal statistical bandwidths, if the available record length is much larger than the segment length. For other measures of bandwidth, such as the half-power bandwidth B, we are led to anticipate this same result. In a later section, we will demonstrate this quantitatively not only for $T/L \gg 1$ but for small values of this ratio as well, and for finite values of P, the number of pieces.

It is of interest to compare Eq. (20) with the results of Blackman and Tukey [2, Secs. B6-B8] for spectral estimation via the "indirect" correlation function approach. Their EDF at frequency f_1 is given approximately by

$$2T\, \frac{\left[\int_0^{\infty} df\, \left[Q_i(f+f_1) + Q_i(f-f_1)\right]\, G(f)\right]^2}{\int_0^{\infty} df\, \left[Q_i(f+f_1) + Q_i(f-f_1)\right]^2\, G^2(f)} \tag{24}$$

for long records, where Q_i is their spectral window. For frequencies f_1 greater than the width of spectral window Q_i, and assuming that Q_i is narrow compared with the finest detail in true spectrum G, Eq. (24) becomes approximately

$$2T\, \frac{\left[\int_0^{\infty} df\, Q_i(f-f_1)\right]^2}{\int_0^{\infty} df\, Q_i^2(f-f_1)}. \tag{25}$$

In order to relate the EDF in Eq. (25) to the one used here, we note that the mean value of Blackman and Tukey's spectral estimate is given by the convolution of Q_i with G. We then identify Q_i with $|W|^2$, obtaining for the EDF in Eq. (25):

$$2T \frac{\left[\int_{-\infty}^{\infty} df\, |W(f)|^2\right]^2}{\int_{-\infty}^{\infty} df\, |W(f)|^4}, \tag{26}$$

which is in agreement with Eq. (20) for long records. Thus, under the assumptions given above, the same limiting value of EDF is realized by both the "indirect" correlation approach and the present "direct" FFT approach; that is, both methods are capable of the same statistical stability if the proper overlap is used in the FFT approach.

DATA WINDOWS AND CHARACTERISTICS

Four data windows will be considered here. They are all continuous; however, they have differing degrees of continuity in their derivatives, leading to different rates of decay of their spectral windows for large frequencies. The triangular data window, made up of two straight-line segments, has a discontinuous first derivative. The cosine data window (Hanning) has a discontinuous second derivative. The quadratic data window is made up of segments of quadratic curves so chosen that the first derivative is everywhere continuous, but the second derivative is discontinuous; thus, the quadratic data window has behavior similar to that of the cosine data window. The cubic data window is made up of segments of cubic curves so chosen that the second derivative is everywhere continuous, but the third derivative is discontinuous. This sequence of windows will have progressively better high-frequency decay and, as will be seen shortly, better side lobes at low frequencies. (Hamming weighting is not considered because its discontinuous data window yields a slowly decaying spectral window for large frequencies.) Computation of the quadratic and cubic data windows is easier and faster than computation of the cosine data window in the time domain.* Their computational advantage and better sidelobe behavior, make them attractive candidates for spectral analysis.

*In the frequency domain, the cosine data window is equivalent to convolution with the sequence -1/4, 1/2, -1/4, which is easily implemented.

The four windows are detailed below in Eqs. (27) through (30). They have been normalized in such a way that $U(0) = 1$. From Eq. (9) and Fig. 1, notice that $u(t) = 0$ for $|t| \geq 1/2$. (The expressions for the correlations ϕ_u of the windows are collected in Appendix B; these correlations are necessary for the evaluation of Eq. (14).) In the following, $\mathrm{sinc}(x) \equiv \sin(\pi x)/(\pi x)$.

Triangular Data Window

$$u(t) = 2\,(1 - 2|t|), \quad |t| \leq \frac{1}{2}$$

$$U(f) = \mathrm{sinc}^2(f/2) \ . \tag{27}$$

Cosine Data Window

$$u(t) = 1 + \cos(2\pi t), \quad |t| \leq \frac{1}{2}$$

$$U(f) = \frac{\mathrm{sinc}(f)}{1 - f^2} \ . \tag{28}$$

Quadratic Data Window

$$u(t) = \begin{cases} \frac{9}{4}\left(1 - 12t^2\right), & |t| \leq \frac{1}{6} \\ \frac{27}{8}\left(1 - 2|t|\right)^2, & \frac{1}{6} \leq |t| \leq \frac{1}{2} \end{cases}$$

$$U(f) = \mathrm{sinc}^3(f/3) \ . \tag{29}$$

Cubic Data Window

$$u(t) = \begin{cases} \frac{8}{3}\left(1 - 24t^2 + 48|t|^3\right), & |t| \le \frac{1}{4} \\ \frac{16}{3}\left(1 - 2|t|\right)^3, & \frac{1}{4} \le |t| \le \frac{1}{2} \end{cases}$$

$$U(f) = \text{sinc}^4(f/4) \ . \tag{30}$$

The function W(f) is available from the normalized function U(f) according to

$$W(f) = L\, U(Lf) \ , \tag{31}$$

upon Fourier transformation of Eq. (9). We define the half-power bandwidth of spectral window $|W|^2$ as the frequency range over which $|W|^2$ is greater than half of its peak value:

$$\left|W\left(\pm \frac{1}{2}B\right)\right|^2 = \frac{1}{2}\left|W(0)\right|^2 . \tag{32}$$

In addition to the statistical-bandwidth constant C_{st} defined in Eq. (21), we define a half-power-bandwidth constant C according to

$$B = \frac{C}{L} \ . \tag{33}$$

Numerical values for both of these dimensionless constants for the four windows are given in Table 1.

The bandwidth constants are larger for the "smoother" data windows; thus, their bandwidths are larger for a given segment length L (Fig. 1). Alternatively, if the bandwidths are to be kept equal for the four windows, the segment lengths must be larger for the smoother data windows.

In the bottom row of Table 1, the ratio of the statistical-bandwidth constant to the half-power-bandwidth constant is found to be relatively constant for the four windows considered. Thus, the statistical stability of the spectral esti-

Table 1

BANDWIDTH CONSTANTS

	Data Window			
	Triangular	Cosine	Quadratic	Cubic
C_{st}	1.854	2.079	2.304	2.686
C	1.276	1.441	1.572	1.820
C_{st}/C	1.454	1.443	1.466	1.476

mates can be discussed in terms of either bandwidth without fear of changing significantly the quantitative aspects. For example, Eq. (22) becomes

$$K_{\alpha} \approx 2.9(T-L)B, \quad \text{for } \frac{T}{L} \gg 1, \tag{34}$$

in terms of half-power bandwidth B, where Eqs. (21) and (33) and Table 1 have been employed. A more precise relation than Eq. (34) will be given for K in the next section, where the number of pieces P will be finite.

Half of each symmetric spectral window is plotted in dB versus f/B in Figs. 3 through 6. Here

$$dB \equiv 10 \log_{10} |U|^2, \tag{35}$$

since the power-density spectrum G is seen through a window proportional to $|U|^2$. All the plots go through -3.01 dB at f/B = 1/2, since B is the half-power bandwidth. The slow spectral decay of the triangular data window and the fast spectral decay of the cubic data window are evident. The cosine and quadratic data windows exhibit intermediate behavior. The first three side lobes of the spectral windows are given in Table 2, where it is seen that the quadratic window offers an 8.3-dB improvement relative to the cosine window in the size of the first side lobe, and the cubic window yields an additional 13.3-dB improvement.

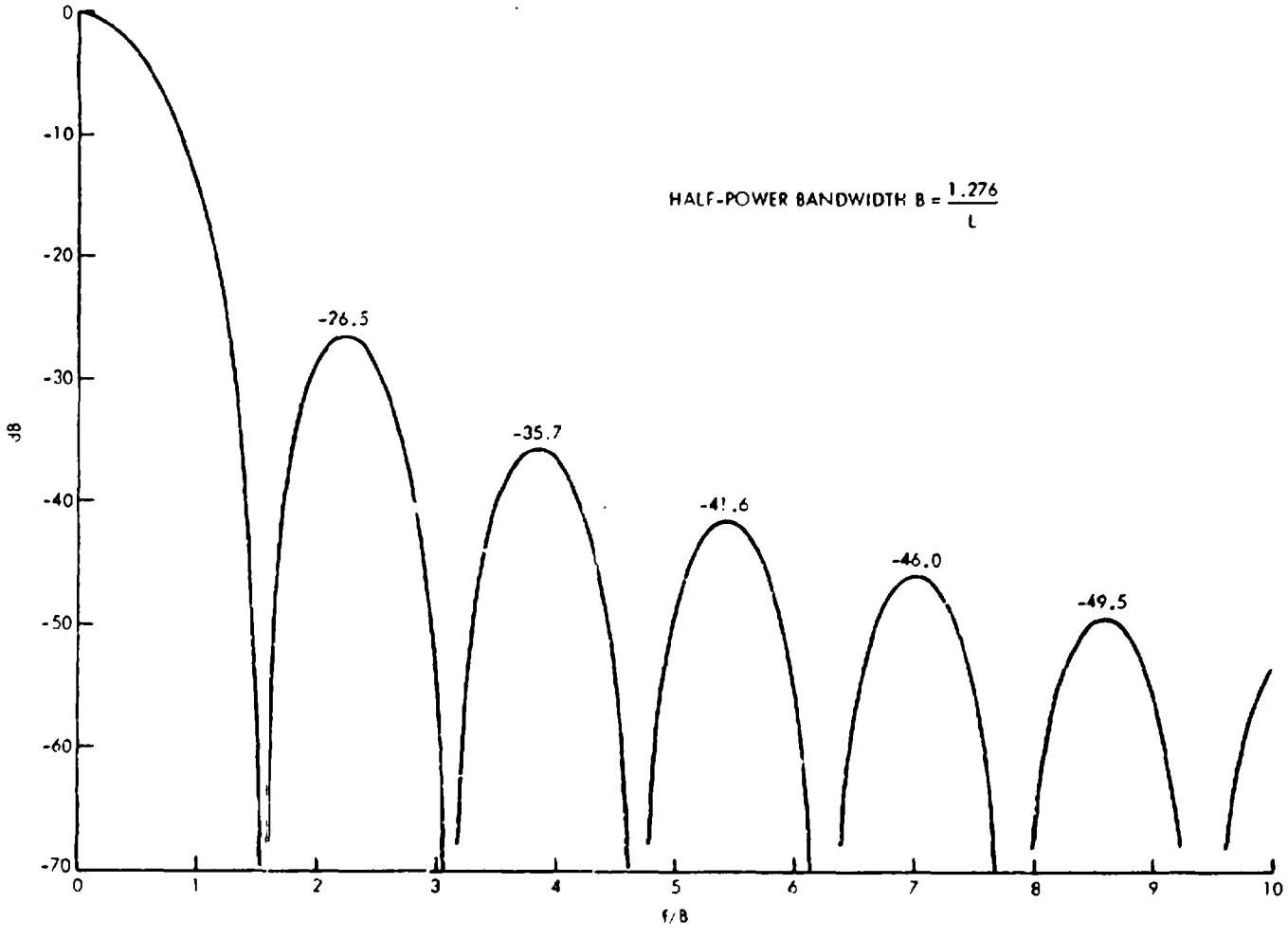

Fig. 3. Spectral Window for Triangular Data Window

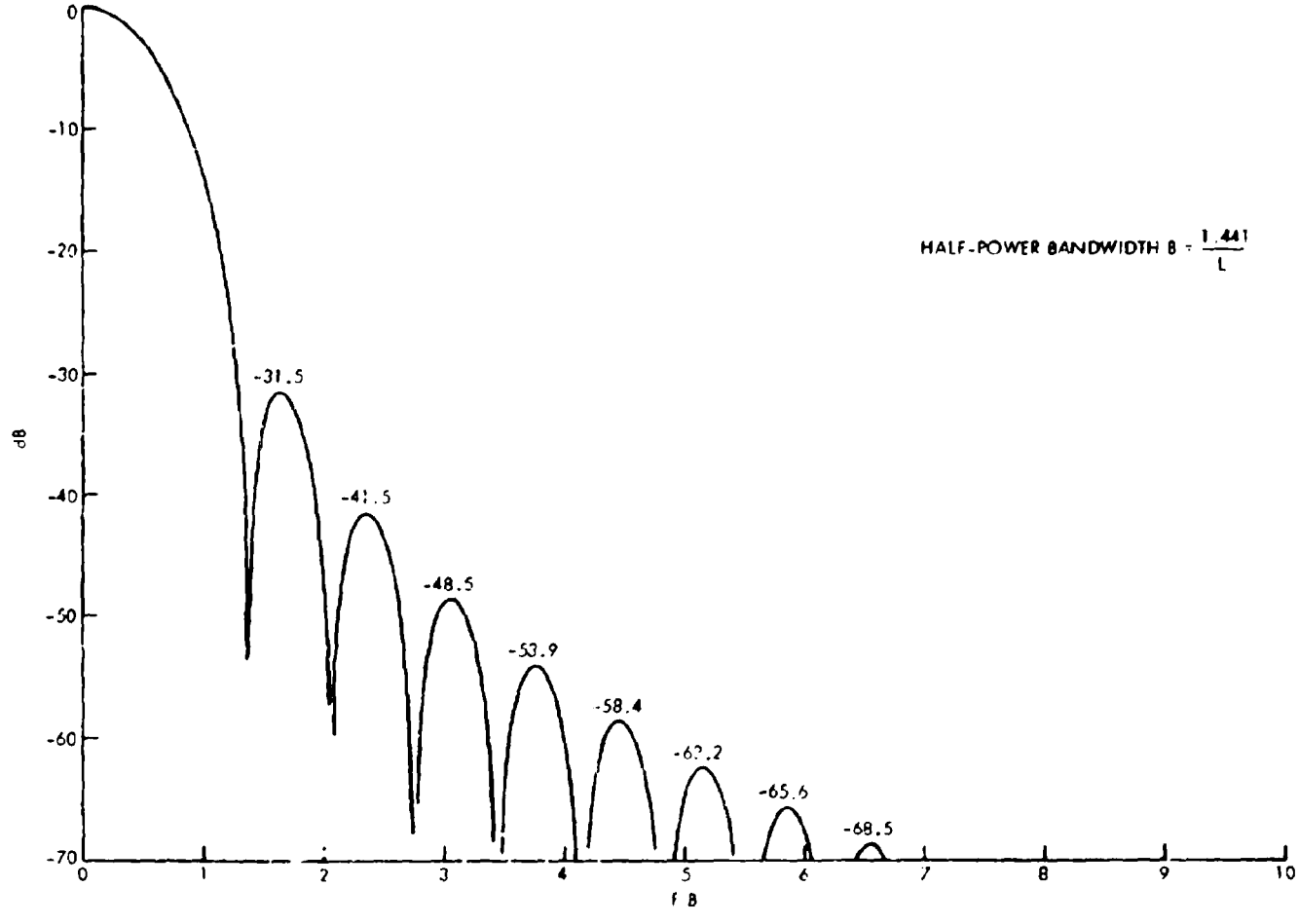

Fig. 4. Spectral Window for Cosine Data Window

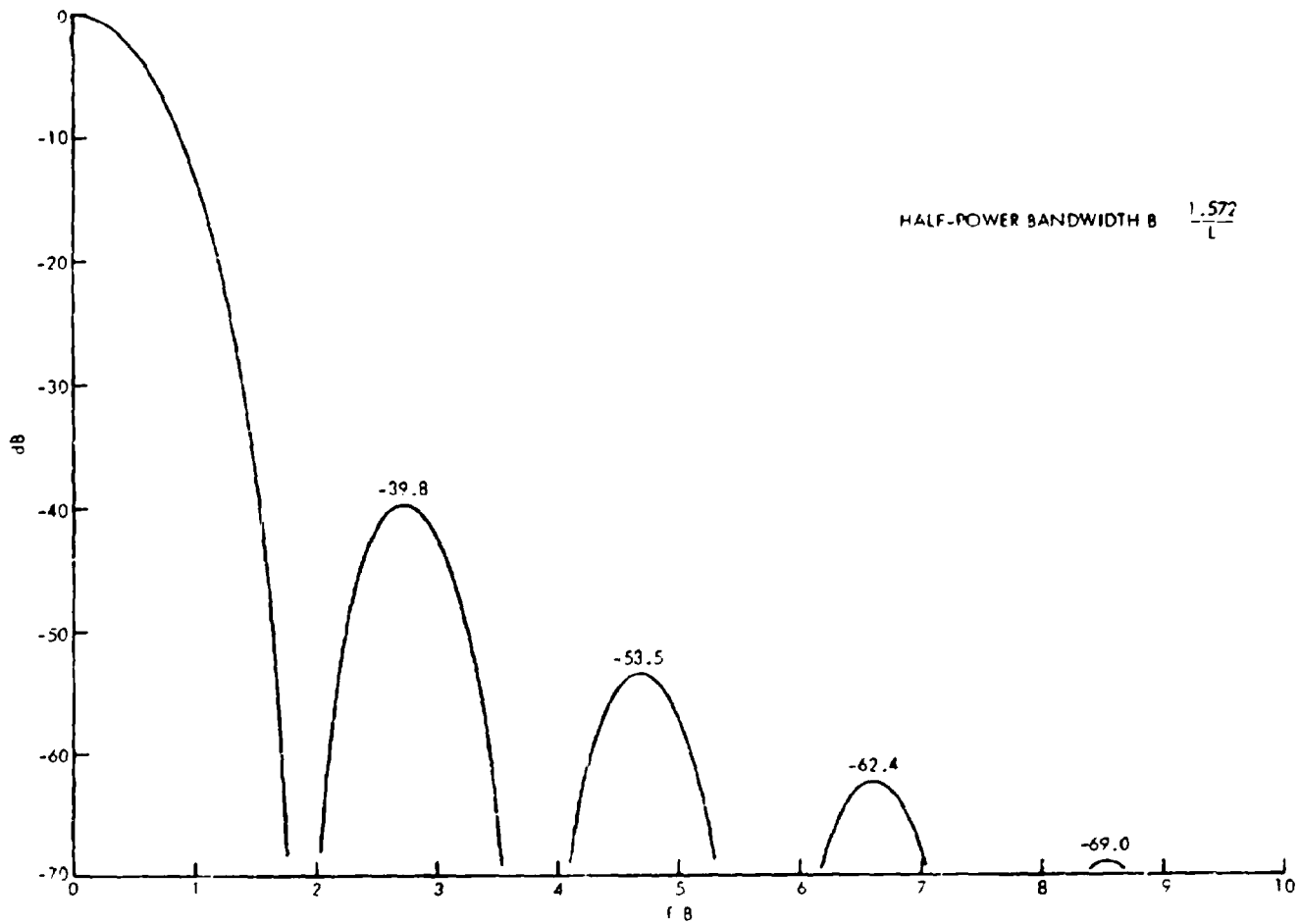

Fig. 5. Spectral Window for Quadratic Data Window

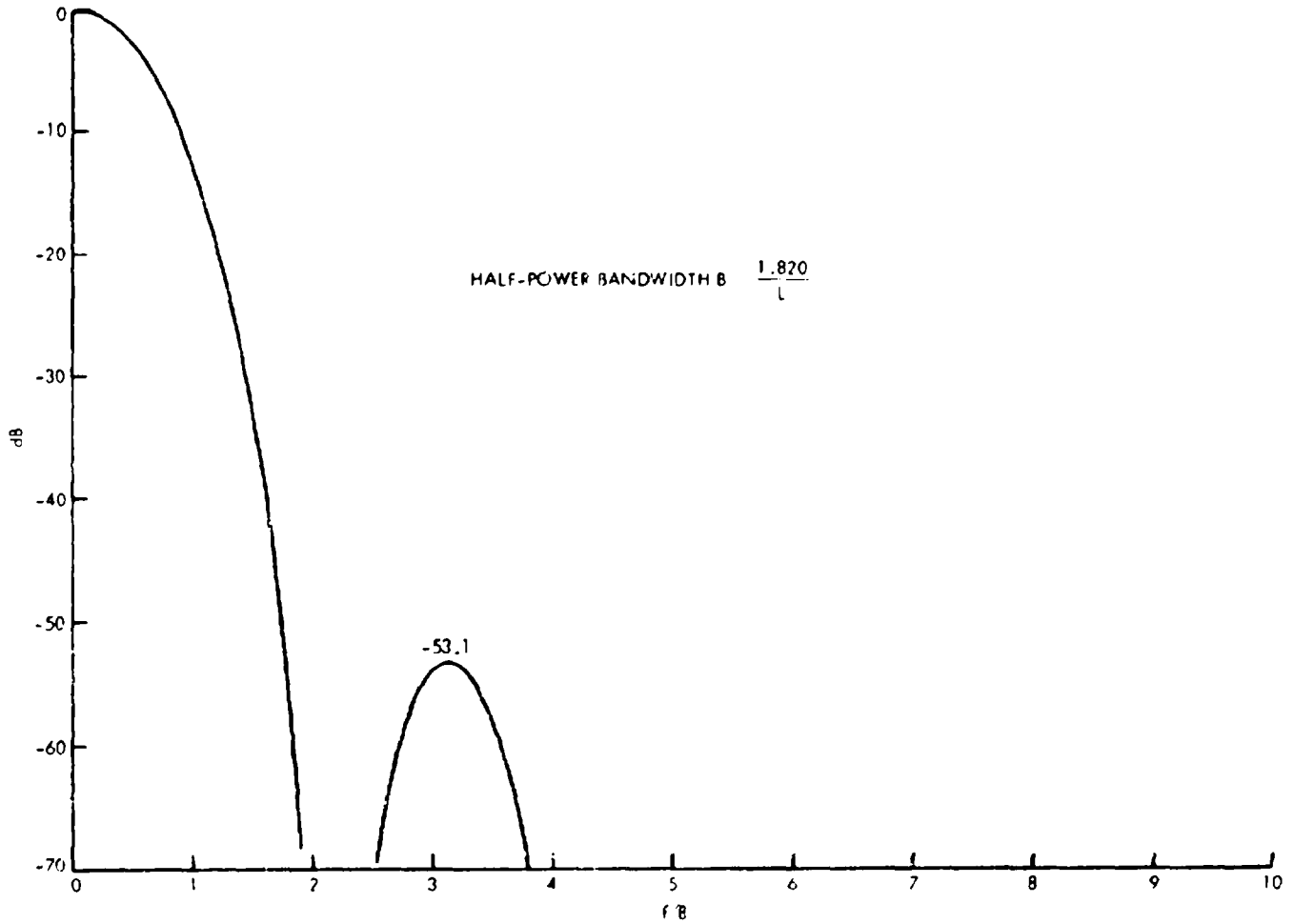

Fig. 6. Spectral Window for Cubic Data Window

Table 2

FIRST THREE SIDE LOBES OF SPECTRAL WINDOWS

Data Window	Side Lobes (dB)		
Triangular	-26.5	-35.7	-41.6
Cosine	-31.5	-41.5	-48.5
Quadratic	-39.8	-53.5	-62.4
Cubic	-53.1	-71.3	-83.2

RESULTS

The general expression for EDF is given in Eq. (14). We eliminate the segment length L in this expression in favor of the half-power bandwidth B by using Eq. (33) to obtain the dependence on the fundamental parameter BT (see Introduction). It follows that

$$K = \frac{2P}{\sum_{k=-(P-1)}^{P-1} \left(1 - \frac{|k|}{P}\right) \left| \frac{\Phi_u\left(k\frac{BT/C-1}{P-1}\right)}{\Phi_u(0)} \right|^2} . \qquad (36)$$

For a particular window u and value of BT, K is computed versus P. A sample tabulation for the cosine data window and BT = 8 is given in Table 3. The column headed "Fractional Overlap" is a measure of how much the individual data windows overlap in the spectral processing technique depicted in Fig. 1 and is given by

Table 3

EQUIVALENT DEGREES OF FREEDOM
VERSUS NUMBER OF PIECES,
BT = 8, COSINE DATA WINDOW

P	K	Fractional Overlap
2	4.00	.00
3	6.00	.00
4	8.00	.00
5	10.00	.00
6	12.00	.09
7	14.00	.24
8	15.96	.35
9	17.74	.43
10	19.13	.49
11	20.03	.54
12	20.50	.59
13	20.69	.62
14	20.73	.65
15	20.71	.67
16	20.66	.70
17	20.61	.72
18	20.56	.73
19	20.52	.75
20	20.48	.76
30	20.19	.84
40	20.04	.88
50	19.95	.91
100	19.77	.95
200	19.67	.98

$$FO = \frac{L-S}{L} = \frac{P-T/L}{P-1} = \frac{P-BT/C}{P-1} \quad , \tag{37}$$

when non-negative. Equations (13) and (33) were employed in Eq. (37).

Several points in Table 3 are worth noting. For no overlap, the EDF increases linearly with P, and even as overlap begins to occur, the rate of increase of EDF remains the same. Thus, 24% overlap still yields the maximum possible EDF for P = 7. However, as P and the overlap increase further, the EDF increases more slowly, eventually reaching a maximum,* after which it decreases slightly for further increases in P. A point of diminishing returns is reached somewhere near P = 12, where 98% of the maximum (max) EDF is realized. The extra computational effort in spectral analysis for P > 12 is not worth the return in stability. The fractional overlap for 98% of max EDF is .59; the EDF is then 20.5, whereas it was only 10.0 for the last non-overlapped example. The case for overlapped processing is well demonstrated by Table 3.

Similar results for all four windows and BT = 2, 4, 8, 16, 32, and 64 are condensed in Table 4, which gives the required number of pieces and the corresponding fractional overlap for a specified fraction of the max EDF. For example, in Table 4B for the cosine data window, in order to realize a specified fraction of 98% of the max EDF at BT = 8, the number of pieces required is 12, and the corresponding fractional overlap is .59. The bottom row of each data-window table gives the max EDF for the corresponding value of BT. Also provided is an equation for max EDF, which was empirically determined to fit through the numerical values obtained.

Several striking invariances are apparent upon inspection of Table 4. First, for a given record length T and desired frequency resolution B, the max

---

* The existence of a finite value of P for maximum EDF is similar to the situation cited in Reference 11.

EDF is virtually independent* of the window employed; that is, all the windows considered have the same variance-reduction capability in spectral estimation when compared under the same frequency-resolution constraint. A simple, approximate rule of thumb for all four windows is given by

$$\max \text{EDF} \approx 3\,(BT - 1). \tag{38}$$

Recall that B is the half-power bandwidth of the spectral window.

For a given window and specified fraction of the max EDF, it will be observed from Table 4 that for $BT > 4$, the required fractional overlap is approximately constant (independent of BT). Therefore, in the last column of Table 4 is entered a representative or "average" fractional overlap required for the specified fraction of max EDF entered in the first column. (This simple rule does not hold well when 100% of the max EDF is required; accordingly, no value is entered for this case.)

For a given value of BT, the number of pieces required to realize .99 (or less) of max EDF is virtually independent of the particular window employed in spectral analysis. This independence is very important; it says that all four windows require the same number of FFTs in order to realize the same EDF and that selection among the [illegible] therefore, can not be based upon the number of FFTs required, [illegible] based upon some other consideration such as side-lobe level or [illegible] (to be discussed). An approximate rule of thumb for the number of p[illegible]uired is given by

$$\text{Number of pieces required} \sim 1.75\,BT \quad \text{for .99 of max EDF.} \tag{39}$$

For large BT products, the number of pieces required to realize max EDF is significantly larger than the number required to realize 99% of max EDF; thus, this large amount of additional processing yields insignificant improvement and is to be avoided.

---

*Very small values of BT are an exception; these are of little practical interest however.

Table 4

NUMBER OF PIECES REQUIRED (P) AND CORRESPONDING FRACTIONAL OVERLAP (FO) FOR A SPECIFIED FRACTION OF THE MAXIMUM EDF

Table 4A. Triangular Data Window

Specified Fraction of max EDF	BT												"Average" Fractional Overlap
	2		4		8		16		32		64		
	P	FO	P	FO	P	FO	P	FO	P	FO	P	FO	
.90	2	.43	5	.47	10	.41	21	.42	43	.43	87	.43	.43
.95	2	.43	5	.47	11	.47	23	.48	48	.49	96	.48	.48
.96	2	.43	5	.47	11	.47	24	.50	49	.50	99	.50	.50
.97	2	.43	6	.57	11	.47	25	.52	50	.51	102	.51	.52
.98	2	.43	6	.57	12	.52	25	.52	52	.53	107	.54	.54
.99	2	.43	6	.57	13	.56	27	.56	56	.56	115	.57	.56
1.00	2	.43	6	.57	14	.59	31	.62	100	.76	211	.77	—
max EDF	3.90		9.74		21.25		44.31		90.68		183.62		

max EDF ≈ 2.91 BT - 2.27

Table 4B. Cosine Data Window

Specified Fraction of max EDF	BT												"Average" Fractional Overlap
	2		4		8		16		32		64		
	P	FO	P	FO	P	FO	P	FO	P	FO	P	FO	
.90	2	.36	5	.56	10	.49	21	.49	43	.51	86	.49	.50
.95	2	.36	5	.56	11	.54	23	.54	47	.54	95	.54	.54
.96	2	.36	5	.56	11	.54	24	.56	48	.55	98	.55	.55
.97	2	.36	5	.56	12	.59	24	.56	50	.57	101	.57	.57
.98	2	.36	5	.56	12	.59	25	.58	52	.58	105	.58	.58
.99	2	.36	6	.64	13	.62	27	.61	55	.61	112	.61	.61
1.00	2	.36	6	.64	14	.65	31	.66	68	.68	146	.70	—
max EDF	3.55		9.24		20.73		43.76		89.87		182.15		

max EDF ≈ 2.88 BT - 2.43

Table 4C. Quadratic Data Window

Specified Fraction of max EDF	BT												"Average" Fractional Overlap
	2		4		8		16		32		64		
	P	FO	P	FO	P	FO	P	FO	P	FO	P	FO	
.90	2	.73	5	.61	10	.55	21	.54	43	.54	88	.54	.54
.95	2	.73	5	.61	11	.59	23	.58	48	.59	98	.59	.59
.96	2	.73	5	.61	11	.59	24	.60	49	.60	100	.60	.60
.97	2	.73	5	.61	12	.63	25	.62	51	.61	104	.61	.62
.98	2	.73	5	.61	12	.63	26	.63	53	.63	108	.63	.63
.99	2	.73	5	.61	13	.66	27	.65	56	.65	115	.65	.65
1.00	2	.73	6	.69	14	.69	32	.70	69	.72	146	.72	—
max EDF	3.10		8.96		20.64		44.05		90.91		184.67		
max EDF ≈ 2.93 BT - 2.87													

Table 4D. Cubic Data Window

Specified Fraction of max EDF	BT												"Average" Fractional Overlap
	2		4		8		16		32		64		
	P	FO	P	FO	P	FO	P	FO	P	FO	P	FO	
.90	2	.90	4	.60	10	.62	21	.61	43	.61	88	.61	.61
.95	2	.90	5	.70	11	.66	23	.65	48	.65	98	.65	.65
.96	2	.90	5	.70	11	.66	24	.66	50	.66	101	.66	.66
.97	2	.90	5	.70	11	.66	25	.68	51	.67	105	.67	.67
.98	2	.90	5	.70	12	.69	26	.69	53	.68	109	.68	.69
.99	2	.90	5	.70	12	.69	27	.70	57	.70	116	.70	.70
1.00	2	.90	5	.70	14	.74	32	.75	70	.76	150	.77	—
max EDF	2.22		8.28		20.03		43.59		90.78		185.18		
max EDF ≈ 2.95 BT - 3.65													

Table 5

REQUIRED FRACTIONAL OVERLAP FOR .99 max EDF

	Data Window			
	Triangular	Cosine	Quadratic	Cubic
Fractional Overlap	.56	.61	.65	.70

The required fractional overlap is greater for the better-side-lobe windows. Thus, for example, to realize .99 of max EDF, we have (virtually independent of the BT product) the values listed in Table 5. Notice that rather large overlaps are required for some windows.

The difficulty of realizing general fractional overlaps, such as .56, raises the question as to what fraction of max EDF is attainable if one restricts overlaps to a few easily realized overlaps such as .50 and .625. This question is answered in Tables 6 and 7.* Table 6 indicates that the cosine data window at 50% overlap (a popular case) yields 92% of the max EDF. However, the cubic data window realizes only 75% of its potential at 50% overlap. Table 7 shows that when the fractional overlap is increased to 5/8, the cosine and quadratic data windows realize virtually their ultimate capability. If the overlap is increased to 75%, the cubic data window then realizes its max EDF.

Table 6

ATTAINABLE FRACTION OF max EDF
AT .50 FRACTIONAL OVERLAP

	Data Window			
	Triangular	Cosine	Quadratic	Cubic
Fraction of max EDF	.96	.92	.85	.75

*These values are not attainable from Table 4 but come from the complete tabular results, of which Table 3 is one example.

Table 7

ATTAINABLE FRACTION OF MAX EDF
AT .625 FRACTIONAL OVERLAP

	Data Window		
	Cosine	Quadratic	Cubic
Fraction of max EDF	1.00	.98	.93

Thus far, no trade-off has been necessary to realize the better side lobes of the smoother data windows; that is, by proper choice of overlap, equal statistical stability is attainable, and an equal number of FFTs is required, for all four windows. However, there is one trade-off that enters as follows: if the original record length T is composed of samples of a process at increments* Δt, more samples are contained in the segment length L for the better-side-lobe windows; that is, the number of samples in interval L is

$$N_s = \frac{L}{\Delta t} = \frac{C}{B\,\Delta t} \quad , \tag{40}$$

employing Eq. (33). N_s is directly proportional to half-power-bandwidth constant C for a specified sampling increment Δt and resolution B. Thus, using Table 1, the cosine data window requires 1.13 times as many samples as the triangular data window requires. The corresponding ratios for the quadratic and cubic data windows are 1.23 and 1.43, respectively. Thus, better side lobes in spectral analysis can be realized at the expense of larger-size FFTs, rather than at the expense of statistical stability or number of FFTs. These comments hold for equal half-power bandwidths of the windows.

For a specified sampling increment Δt, desired resolution B, and particular window, Eq. (40) will generally not be a power of 2. Since FFTs run

*The sampling increment Δt must be chosen small enough to avoid aliasing; this is the only area where the bandwidth of the process comes into consideration.

faster when conducted at powers of 2, it is recommended that the desired resolution B be changed somewhat (increased or decreased) so as to make N_s a power of 2. This is generally a tolerable situation since B is often a "guesstimate" in the first place.

OPTIMUM WEIGHTING OF INDIVIDUAL SPECTRAL ESTIMATES

In Eq. (3), the p-th estimate $|Y_p(f)|^2$ of the power-density spectrum was weighted equally with all other estimates. In this section, we consider whether unequal weighting will yield additional worthwhile variance reduction. Inasmuch as the edge pieces in Fig. 1 are weighted only once by a data window, whereas the interior pieces are weighted more than once, perhaps heavier weighting of the edge pieces will yield additional stability. The power-density estimate is formed as

$$\tilde{G}(f) = \sum_{p=1}^{P} w_p \left| Y_p(f) \right|^2. \tag{41}$$

The derivation of the EDF of this estimate is given in Appendix C, which also presents the optimization of the EDF by choice of weights for a given P, record length, and window. A summary of the numerical results is given in Table 8, where P is varied up to 64. The largest value of EDF attained over that range of P is quoted in Table 8, except for BT = 16 where, with the exception of the triangular data window, P = 64 was not yet great enough to reach the max EDF by weighting.

Table 8

OPTIMUM EDF VALUES

Data Window	BT			
	2	4	8	16
Triangular	4.37	10.12	21.65	44.72
Cosine	4.50	10.15	21.44	>43.87
Quadratic	4.07	9.80	21.29	>44.18
Cubic	3.82	9.52	20.94	>43.72

A comparison of Table 8 with the max EDF values of Fig. 4 reveals that very little is to be gained by optimum weighting, except for small values of BT. However, small values of BT are not of great practical interest because the estimates are very unstable statistically. Also, the number of pieces P required to realize the optimum EDF is rather large; for example, in order to gain an improvement in EDF of 0.5 over the max EDF in Table 4, 19 pieces are required for the cosine data window, 20 pieces for the quadratic data window, and 15 pieces for the cubic data window. Moreover, the optimum weights are found to alternate in sign for some cases, causing a loss in significance.

DISCUSSION

This investigation of four good data windows indicates that there is no best window for spectral estimation. Rather, there is a trade-off to be made when choosing a window: the better-side-lobe windows require larger-size FFTs. When the proper overlap is used for each data window, the selection of windows can not be made on the basis of statistical stability or the number of FFTs required.

The quadratic and cubic data windows are simpler and quicker to compute than the cosine data window in the time domain (but not in the frequency domain as regards their effects). In addition, the quadratic and cubic windows have better side-lobe behavior and, therefore, merit serious consideration for spectral analysis. However, they require larger-size (but not more) FFTs than does the cosine data window.

The reason that the better-side-lobe windows do not require more FFTs than do the other windows is as follows. For a fixed half-power bandwidth B, the better-side-lobe windows require larger segment lengths L; however, the corresponding data windows tend to be more peaked near the center of the segment length. In order to utilize a given record length for maximum statistical stability, these data windows must, therefore, overlap for a greater percentage of the segment length. It turns out that the increased segment length and increased overlap almost exactly compensate each other, so that a constant number of FFTs is required regardless of the window selection.

This report has concentrated on the variance of the spectral estimates. In Appendix D, it is shown that the covariance of spectral estimates at two different frequencies is always positive but is essentially zero when the frequencies differ by more than the width of the spectral window. Thus, spectral estimates at frequencies farther apart than B are statistically linearly independent of each other.

Appendix A

DERIVATION OF MEAN AND VARIANCE

From Eqs. (2) and (3), the spectral estimate at frequency f is

$$\hat{G}(f) = \frac{1}{P}\sum_{p=1}^{P}\iint du\, dv\, \exp\left(-i2\pi f(u-v)\right)\, x(u)x^*(v) \cdot$$

$$w\left[u - \frac{L}{2} - (p-1)S\right]\, w^*\left[v - \frac{L}{2} - (p-1)S\right] . \qquad (A-1)$$

(For completeness, process x and window w are allowed to be complex.) The mean value of $\hat{G}(f)$ is obtained by ensemble-averaging Eq. (A-1) over the possible realizations of process x. Expressing the correlation of x as a Fourier transform of spectrum G, we find the average value

$$E\left\{\hat{G}(f)\right\} = \frac{1}{P}\sum_{p=1}^{P}\iint du\, dv\, \exp\left(-i2\pi f(u-v)\right)\int d\nu\, \exp\left(i2\pi(u-v)\nu\right)\, G(\nu) \cdot$$

$$w\left[u - \frac{L}{2} - (p-1)S\right]\, w^*\left[v - \frac{L}{2} - (p-1)S\right]$$

$$= \int d\nu\, G(\nu)\left|W(f-\nu)\right|^2 = \int d\nu\, G(f-\nu)\left|W(\nu)\right|^2 , \qquad (A-2)$$

where we have utilized Eq. (4). If spectral window $|W|^2$ is narrower than the finest detail in the true spectrum G, Eq. (A-2) becomes

$$E\left\{\hat{G}(f)\right\} \cong G(f)\int d\nu\, \left|W(\nu)\right|^2 . \qquad (A-3)$$

Equation (A-2) is not limited to Gaussian processes but is, in fact, true for any stationary process.

In order to evaluate the variance of the spectral estimate, we start with

$$E\{\hat{G}^2(f)\} = \frac{1}{P^2}\sum_{p=1}^{P}\sum_{q=1}^{P}\iiiint du\,dv\,dr\,ds\,\exp\left(-i2\pi f(u-v+r-s)\right)\,E\{x(u)x^*(v)x(r)x^*(s)\}\cdot$$

$$w\left[u-\frac{L}{2}-(p-1)S\right]\,w^*\left[v-\frac{L}{2}-(p-1)S\right]\,w\left[r-\frac{L}{2}-(q-1)S\right]\,w^*\left[s-\frac{L}{2}-(q-1)S\right]\,, \tag{A-4}$$

In order to simplify this expression, we must be able to evaluate the fourth-order average. If x is a real Gaussian random process, the average in Eq. (A-4) becomes

$$R(u-v)\,R(r-s)+R(u-r)\,R(v-s)+R(u-s)\,R(r-v)\,, \tag{A-5}$$

where R is the correlation of process x. (If x is a complex envelope of a Gaussian process, the middle term in Eq. (A-5) is absent [12].) When we express correlation R as a Fourier transform of spectrum G and substitute Eq. (A-5) in Eq. (A-4), we obtain

$$E\{\hat{G}^2(f)\} = \frac{1}{P^2}\sum_{p=1}^{P}\sum_{q=1}^{P}\iiiint du\,dv\,dr\,ds\,\exp\left(-i2\pi f(u-v+r-s)\right)\cdot$$

$$w\left[u-\frac{L}{2}-(p-1)S\right]\,w^*\left[v-\frac{L}{2}-(p-1)S\right]\,w\left[r-\frac{L}{2}-(q-1)S\right]\,w^*\left[s-\frac{L}{2}-(q-1)S\right]\cdot$$

$$\iint d\mu\,d\nu\,G(\mu)\,G(\nu)\,\left[\exp\left(i2\pi\mu(u-v)+i2\pi\nu(r-s)\right)+\exp\left(i2\pi\mu(u-r)+i2\pi\nu(v-s)\right)\right.$$

$$\left.+\exp\left(i2\pi\mu(u-s)+i2\pi\nu(r-v)\right)\right]$$

$$=\frac{1}{P^2}\sum_{p=1}^{P}\sum_{q=1}^{P}\iint d\mu\,d\nu\,G(\mu)\,G(\nu)\,\left[|W(f-\mu)|^2\,|W(f-\nu)|^2+\exp(i2\pi(\mu-\nu)(p-q)S)\cdot\right.$$

$$\left.W(f-\mu)\,W^*(f+\nu)\,W(f+\mu)\,W^*(f-\nu)+\exp(i2\pi(\mu-\nu)(p-q)S)\,|W(f-\mu)|^2\,|W(f-\nu)|^2\right]\,, \tag{A-6}$$

using Eq. (4). The first term in Eq. (A-6) is recognized from Eq. (A-2) as the square of the mean of $\hat{G}$. Therefore,

$$\mathrm{Var}\{\hat{G}(f)\} = \frac{1}{P^2}\sum_{p=1}^{P}\sum_{q=1}^{P}\left|\int d\mu\, G(\mu)\, \exp(i2\pi\mu(p-q)S)\, W(f-\mu)\, W(f+\mu)\right|^2$$

$$+\frac{1}{P^2}\sum_{p=1}^{P}\sum_{q=1}^{P}\left|\int d\mu\, G(\mu)\, \exp(i2\pi\mu(p-q)S)\, |W(f-\mu)|^2\right|^2 . \quad (A-7)$$

Now if f, the frequency of interest, is greater than the bandwidth of the spectral window $|W|^2$ (i.e., a couple of resolution cells away from the origin), then $W(f-\mu)$ and $W(f+\mu)$ do not overlap significantly. Letting B be the half-power bandwidth of the spectral window $|W|^2$, we therefore have the excellent approximation* for $f > B$,

$$\mathrm{Var}\{\hat{G}(f)\} \cong \frac{1}{P^2}\sum_{p=1}^{P}\sum_{q=1}^{P}\left|\int d\mu\, G(\mu)\, \exp(i2\pi\mu(p-q)S)\, |W(f-\mu)|^2\right|^2 . \quad (A-8)$$

(For $f = 0$, the two terms in Eq. (A-7) are equal if data window w is real, in which case $\mathrm{Var}\{\hat{G}(0)\}$ is double that given by Eq. (A-8) at $f = 0$.) Making the change of variable $k = p-q$ in Eq. (A-8), we obtain

$$\mathrm{Var}\{\hat{G}(f)\} \cong \frac{1}{P}\sum_{k=-(P-1)}^{P-1}\left(1 - \frac{|k|}{P}\right)\left|\int d\mu\, \exp(i2\pi\mu kS)\, G(\mu)\, |W(f-\mu)|^2\right|^2 . \quad (A-9)$$

But if the bandwidth B of spectral window $|W|^2$ is narrower than the finest detail in spectrum G, the integral on μ in Eq. (A-9) can be approximated by

$$G(f)\int d\mu\, \exp(i2\pi\mu kS)\, |W(f-\mu)|^2$$

$$= G(f)\, \exp(i2\pi fkS)\, \phi_w^*(kS) , \quad (A-10)$$

where we have utilized Eqs. (4) and (7). Then Eq. (A-9) becomes

*When x is a complex envelope, Eq. (A-8) is exact; see comment under Eq. (A-5).

$$\mathrm{Var}\{\hat{G}(f)\} \cong G^2(f)\frac{1}{P}\sum_{k=-(P-1)}^{P-1}\left(1-\frac{|k|}{P}\right)\left|\phi_w(kS)\right|^2 \quad . \qquad \text{(A-11)}$$

This equation is similar to that given in [9, p. 71].

Equations (A-3) and (A-11) are the main products of this appendix.

Appendix B

CORRELATIONS OF DATA WINDOWS

The correlation of the normalized data window u is given by Eq. (11) as

$$\phi_u(\tau) = \int dt\, u(t)\, u^*(t-\tau) \,. \tag{B-1}$$

This quantity is required for the calculation of EDF, K, in Eq. (14). Since $u(t) = 0$ for $|t| \geq 1/2$, then $\phi_u(\tau) = 0$ for $|\tau| \geq 1$. Thus, for the:

Triangular Data Window

$$\frac{\phi_u(\tau)}{\phi_u(0)} = \left\{ \begin{array}{ll} 1 - 6\tau^2 + 6|\tau|^3, & |\tau| \leq \frac{1}{2} \\ 2\,(1 - |\tau|)^3, & \frac{1}{2} \leq |\tau| \leq 1 \end{array} \right\} . \tag{B-2}$$

Cosine Data Window

$$\frac{\phi_u(\tau)}{\phi_u(0)} = \frac{2}{3}(1 - |\tau|)\left[1 + \frac{1}{2}\cos(2\pi\tau)\right] + \frac{1}{2\pi}\sin(2\pi|\tau|), \quad |\tau| \leq 1 \,. \tag{B-3}$$

Quadratic Data Window

$$\frac{\phi_u(\tau)}{\phi_u(0)} = \left\{ \begin{array}{ll} \frac{81}{22}(1 - |\tau|)^5 \equiv Q_1(\tau), & \frac{2}{3} \leq |\tau| \leq 1 \\ Q_1(\tau) - \frac{243}{11}\left(\frac{2}{3} - |\tau|\right)^5 \equiv Q_2(\tau), & \frac{1}{3} \leq |\tau| \leq \frac{2}{3} \\ Q_2(\tau) + \frac{1215}{22}\left(\frac{1}{3} - |\tau|\right)^5, & |\tau| \leq \frac{1}{3} \end{array} \right\} . \tag{B-4}$$

Cubic Data Window

$$\frac{\phi_u(\tau)}{\phi_u(0)} = \left\{ \begin{array}{l} \frac{1024}{151}(1-|\tau|)^7 \equiv C_1(\tau), \quad \frac{3}{4} \le |\tau| \le 1 \\ C_1(\tau) - \frac{8192}{151}\left(\frac{3}{4}-|\tau|\right)^7 \equiv C_2(\tau), \quad \frac{1}{2} \le |\tau| \le \frac{3}{4} \\ C_2(\tau) + \frac{28672}{151}\left(\frac{1}{2}-|\tau|\right)^7 \equiv C_3(\tau), \quad \frac{1}{4} \le |\tau| \le \frac{1}{2} \\ C_3(\tau) - \frac{57344}{151}\left(\frac{1}{4}-|\tau|\right)^7, \quad |\tau| \le \frac{1}{4} \end{array} \right\} . \qquad \text{(B-5)}$$

The forms for the correlation of the quadratic and cubic data windows are compact and very useful for computer programming.

Appendix C

OPTIMUM WEIGHTS FOR EDF

The estimate of the power-density spectrum is given by Eq. (41). By generalizing the results in Appendix A, we have

$$\mathrm{Var}\{\tilde{G}(f)\} \cong \sum_{k=-(P-1)}^{P-1} \gamma_k \left| \int d\mu \, \exp(i2\pi\mu kS) \, G(\mu) \, |W(f-\mu)|^2 \right|^2 , \qquad (C-1)$$

where

$$\gamma_k = \sum_q w_{q+k} \, w_q^* . \qquad (C-2)$$

The sum is over all non-zero terms. Utilizing the same assumptions used in Appendix A, we have

$$\mathrm{Var}\{\tilde{G}(f)\} \cong G^2(f) \sum_{k=-(P-1)}^{P-1} \gamma_k \left| \phi_w(kS) \right|^2 , \qquad (C-3)$$

$$E\{\tilde{G}(f)\} \cong G(f) \sum_p w_p \, \phi_w(0) , \qquad (C-4)$$

yielding

$$\tilde{K} = 2 \frac{\left| \sum_p w_p \right|^2}{\sum_{k=-(P-1)}^{P-1} \gamma_k M_k} , \qquad (C-5)$$

where

$$M_k \equiv \left| \frac{\phi_w(kS)}{\phi_w(0)} \right|^2 = M_{-k} \, . \tag{C-6}$$

Partially differentiating $\tilde{K}$ with respect to w_j^* [13, Appendix] and noting that the absolute scale of weights $\{w_p\}$ does not enter in $\tilde{K}$, we see that the optimum weights must satisfy the equation

$$\sum_k M_k \, w_{j+k} = 1, \quad 1 \le j \le P \, . \tag{C-7}$$

If we define the matrices

$$M = \left[M_{m-n} \right], \quad 1 \le m, n \le P \, ,$$

$$1^T = [1 \; 1 \; \ldots \; 1], \; w^T = [w_1 \; w_2 \; \ldots \; w_P] \, , \tag{C-8}$$

then the optimum weights are

$$w = M^{-1} 1 \, , \tag{C-9}$$

and the optimum EDF is

$$\tilde{K} = 2 \; 1^T M^{-1} 1 \, . \tag{C-10}$$

Appendix D

COVARIANCE OF SPECTRAL ESTIMATES

A generalization of the technique in Appendix A leads to the following expression for the covariance between spectral estimates at frequencies f_1 and f_2:

$$\mathrm{Cov}\{\hat{G}(f_1),\ \hat{G}(f_2)\} = \frac{1}{P^2}\sum_{p=1}^{P}\sum_{q=1}^{P}\left|\int d\mu\ G(\mu)\ W(f_1-\mu)\ W(f_2+\mu)\ \exp(i2\pi\mu(p-q)S)\right|^2$$

$$+\frac{1}{P^2}\sum_{p=1}^{P}\sum_{q=1}^{P}\left|\int d\mu\ G(\mu)\ W(f_1-\mu)\ W^*(f_2-\mu)\ \exp(i2\pi\mu(p-q)S)\right|^2 . \tag{D-1}$$

Now if f_1+f_2 is greater than the bandwidth of the spectral window, $W(f_1-\mu)$ and $W(f_2+\mu)$ are essentially non-overlapping. Then,

$$\mathrm{Cov} \cong \frac{1}{P}\sum_{k=-(P-1)}^{P-1}\left(1-\frac{|k|}{P}\right)\left|\int d\mu\ G(\mu)\ W(f_1-\mu)\ W^*(f_2-\mu)\ \exp(i2\pi\mu kS)\right|^2 . \tag{D-2}$$

This quantity is always positive. However, it is very small when $|f_2-f_1|>B$ because $W(f_1-\mu)$ and $W(f_2-\mu)$ do not overlap then.

When true spectrum G varies but slightly over a frequency range B,

$$\mathrm{Cov} \cong G(f_1)\ G(f_2)\sum_{k=-(P-1)}^{P-1}\left(1-\frac{|k|}{P}\right)\left|\chi(kS,\ f_2-f_1)\right|^2 , \tag{D-3}$$

where

$$\chi(\tau,f) \equiv \int d\mu \exp(i2\pi\mu\tau)\, W(\mu+f)W^*(\mu)$$

$$= \int dt \exp(-i2\pi ft)\, w(t)\, w^*(t-\tau) \qquad \text{(D-4)}$$

is the ambiguity function of window w. Again, if $|f_1-f_2| > B$, Eq. (D-3) is essentially zero, as shown by the first form in Eq. (D-4).

As an example, for the cosine window and 0% overlap, the covariance coefficient (ratio of Cov to the square-root of the product of variances) is $1, \frac{4}{9}, \frac{1}{36}, 0, 0, \ldots,$ for $|f_2-f_1| = 0, \frac{1}{L}, \frac{2}{L}, \frac{3}{L}, \frac{4}{L}, \ldots,$ respectively. Thus spectral estimates $\frac{2}{L}$ Hz apart are essentially uncorrelated. For 50% overlap (and large P), the corresponding covariance coefficients are slightly larger, being 1, .495, .068, .005, 0, ...

REFERENCES

1. M. S. Bartlett, An Introduction to Stochastic Processes, with Special Reference to Methods and Applications, Cambridge University Press, Cambridge, 1953.

2. R. B. Blackman and J. W. Tukey, The Measurement of Power Spectra from the Point of View of Communications Engineering, Dover Publications, Inc., New York, 1959.

3. E. Parzen. "Mathematical Considerations in the Estimation of Spectra," Technometrics, vol. 3, 1961, p. 167.

4. R. B. Blackman, Data Smoothing and Prediction, Addison-Wesley Publishing Company, Inc., Reading, Mass., 1965.

5. J. S. Bendat and A. G. Piersol, Measurement and Analysis of Random Data, J. Wiley & Sons, Inc., New York, 1966.

6. G. M. Jenkins and D. G. Watts, Spectral Analysis and Its Applications, Holden-Day Company, San Francisco, 1968.

7. IEEE Transactions on Audio and Electroacoustics, Special Issue on Fast Fourier Transform, vol. AU-15, no. 2, June 1967.

8. IEEE Transactions on Audio and Electroacoustics, Special Issue on Fast Fourier Transform, vol. AU-17, no. 2, June 1969.

9. P. D. Welch, "The Use of FFT for the Estimation of Power Spectra: a Method Based on Time Averaging over Short Modified Periodograms," IEEE Transactions on Audio and Electroacoustics, vol. AU-15, no. 2, June 1967, pp. 70-73.

10. C. Bingham, M. D. Godfrey, and J. W. Tukey, "Modern Techniques of Power Spectrum Estimation," IEEE Transactions on Audio and Electroacoustics, vol. AU-15, no. 2, June 1967.

11. H. T. Balch et al., "Estimation of the Mean of a Stationary Random Process by Periodic Sampling," Bell System Technical Journal, May-June 1966, pp. 733-741.

12. A. H. Nuttall, "High-Order Covariance Functions for Complex Gaussian Processes," IEEE Transactions on Information Theory, vol. IT-8, no. 3, April 1962, pp. 255-256.

13. A. H. Nuttall, "Trigonometric Smoothing and Interpolation of Sampled Complex Functions, via the FFT," NUSC Technical Memorandum No. TC-94-71, 19 April 1971.